Electronic Supplementary Material (ESI) for Physical Chemistry Chemical Physics

Supplemental Information

Simulated swelling during low temperature N_2 adsorption in polymers of intrinsic microporosity

Kyle E. Hart,[†] Jeffrey M. Springmeier,[†] Neil B. McKeown,[‡] and Coray M. Colina[*,†]

Department of Materials Science and Engineering, The Pennsylvania State University, University Park, PA 16802, and School of Chemistry, Cardiff University, Cardiff, CF10 3AT, U.K.

E-mail: colina@matse.psu.edu

Contents

1 Overview **2**

2 Molecular Models **2**
2.1 PIM-1 . . . 4
2.2 PIM-1c . . . 5
2.3 sPIM-1 . . . 6
2.4 PIM-SBF . . . 7
2.5 PIM-SBF-Me . . . 8

3 Effective Swelling **9**

4 Characterization **10**
4.1 Radial distribution functions . . . 10
4.2 Structure factors . . . 11
4.3 Pore Size Distributions . . . 12
4.4 Curling Angle Distributions . . . 13
4.5 Spiro-Angle Distributions . . . 14
4.6 N_2 adsorption . . . 15
4.7 N_2 adsorption enthalpy . . . 17

[*]To whom correspondence should be addressed
[†]The Pennsylvania State University
[‡]Cardiff University

1 Overview

Shown in this supplemental information is information on the molecular models used, an example script for the effective swelling procedure and all characterization of each simulated sample of each PIM.

2 Molecular Models

The molecular model used to simulated the polymers of intrinsic microporosity in this work uses three distinct interaction potentials: 1) ab initio derived atomic partial charges (Coulombic), 2) bonded interactions and 3) van der Waals interactions. To calculated the partial charges, density functional theory calculations were performed using the B3LYP/6-31 g (d,p) for accurate geometry optimization of the designated symmetric repeat unit. Then, to determine the electrostatic potential (ESP) of the monomer, quantum mechanical calculations at the HF/6-31G* level of theory were run, followed by a restrained electrostatic potential (RESP)[1] charge fitting to map the electrostatic potential to a discrete partial charge distribution that accurately represented the repeat unit's electron density. Charge groups and equivalences were used to maintain symmetry of the repeat unit and charge neutrality. For example, the green highlighted groups of the repeat unit of PIM-SBF (Figure 4b) were restricted to be a charge neutral group such that when they are deleted in the construction of the polymer, charge neutrality is maintained. For all united atom beads, the partial charge of the carbon and associated hydrogens were added together to determine the charge of the bead. Lastly, we use the generalized amber force field (GAFF)[2] for bonded interactions, and the transferable potential for phase equilibria for non-bonded interactions.[3–9]

A naming scheme is used in this work for each united atom bead, similar to previous works.[10] The naming scheme used is: [element][type][hydrogens], where type describes the chemical environment (A = **a**romatic, H = tetra**h**edral, L = **l**inear, P = trigonal **p**lanar, S = **s**hared aromatic, K = **k**etone) and hydrogen specifies the number of bonded hydrogen atoms. For example, CH2 is a tetrahedral carbon unit atom bead with two associated hydrogens. An "L" preceeding an atom type designates a ***l****inker atom* used in the bonding.

The simulation technique *Polymatic* was used to construct the polymers in this work. A three-dimensional periodic cubic box was packed with approx. 100 monomer repeat units. Using the *Polymatic* open source code, the monomers were artificially bonded together until no more bonds could be formed in a reasonable amount of time. All the details of the Polymatic technique can be found in Abbott et al.[10] A sample input script, example shown below, was used for the polymerization input script of PIM-SBF which was used to construct the boxes.

```
cutoff 6.0
link LOA0,OA0 LCS0,CS0
charge -0.3 +0.3
bond 12 4
plane 6,3,7,11 5,2,4,8 <40,>140,||
vector 3,10 2,9 >135
connect
1 3
2 4,5
```

```
3 6,7
4 8
5 9
6 10
7 11,12
types
1 LOA0
2 LCS0
3 CS0
4 LCS0
5 CA0
6 CA1
7 CS0
8 CA0
9 CS0
10 CA0
11 CA1
12 LOA0
```

After the polymers were constructed at a low density (~ 0.5 g/cm^3), the boxes were subjected to the 21-step compression and relaxation scheme, which has been shown to generate predictive boxes with experimental-like densities of polymers,[10–13] and discrete molecules.[14,15] The compression scheme was performed in LAMMPS[16] using the following parameters: $P_{max} = 5 \times 10^4$ bar; $P_{final} = 1$ bar; $T_{max} = 600$ K; and $T_{final} = 300$ K. A sample LAMMPS input script to run the 21-step MD compression and relaxation scheme can be found in Abbott et al.[10]

Listed below are the simulation details of each sample set of PIMs including: (a) the porosity at all swellings (geometric surface area, box length, void volume, bulk density), (b) the details of each of the five boxes in the sample set (number of united atoms and weight-averaged molecular weight of the polymers in the box) Also shown are the generalized amber force field atom definition, the Transferable Potential for Phase Equilibria type definition and parameters, and the ab initio calculated partial charge for each united atom type in each polymer.

2.1 PIM-1

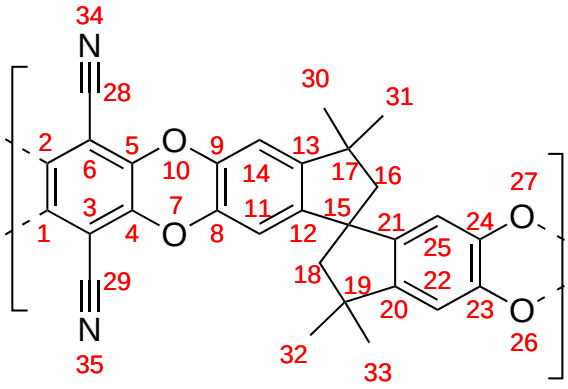

Figure S1: The chemical structure of PIM-1.

Table S1: Simulation details of PIM-1.

(a) Porosity properties of the PIM-1 at all swellings

swelling (%)	SA_{geo} ($m^2 g^{-1}$)	L (Å)	φ ($cm^3 g^{-1}$)	ρ_{bulk} (g cm^{-3})
0	594 ± 84	44.5 ± 0.5	0.447 ± 0.018	0.933 ± 0.016
2	623 ± 61	44.9 ± 0.5	0.468 ± 0.019	0.914 ± 0.016
4	713 ± 93	45.2 ± 0.5	0.490 ± 0.019	0.896 ± 0.015
6	795 ± 83	45.5 ± 0.5	0.512 ± 0.020	0.879 ± 0.016
9	911 ± 74	45.9 ± 0.5	0.545 ± 0.020	0.853 ± 0.015
12	1031 ± 86	46.4 ± 0.5	0.579 ± 0.021	0.829 ± 0.014
15	1148 ± 119	46.8 ± 0.5	0.614 ± 0.022	0.806 ± 0.014

(b) Details of each simulation box of PIM-1

sample	No. of United Atoms	M_w (g/mol)
1	3745	5401
2	3885	5347
3	3710	6029
4	3745	4385
5	3815	4955

Table S2: Force field parameters of PIM-1. Reprinted (adapted) with permission from Larsen et al.[11] Copyright 2011 American Chemical Society.

		GAFF equivalence		TraPPE-UA equivalence		
Atom No.	Atom type	Atom type	Ref.	Atom type	Ref.	Atomic Charge
1, 2, 4, 5	CS0	ca	2	**C**(aro link)	3	0.172261
3, 6	CA0	ca	2	R–**C**(aro)	3	-0.123040
7, 10, 26, 27	OA0	os	2	C(aro)–**O**(aro)–C(aro)	4	-0.219064
9, 8, 23, 24	CS0	ca	2	**C**(aro link)	3	0.177839
11, 14, 22, 25	CA1	ca	2	**CH**(aro)	3	-0.124962
12, 13, 20, 21	CA0	ca	2	R–**C**(aro)	3	0.0383560
15	CH0	c3	2	**C**	6	0.0979454
17, 19	CH0	c3	2	**C**	6	0.0979454
16, 18	CH2	c3	2	$\mathbf{CH_2}$	5	-0.0164660
28, 29	CL0	c1	2	**C**(*sp*)	7	0.313718
34, 35	NL0	n1	2	**N**(nitrile)	7	-0.409990
30, 31, 32, 33	CH3	c3	2	$\mathbf{CH_3}$	5	0.0

2.2 PIM-1c

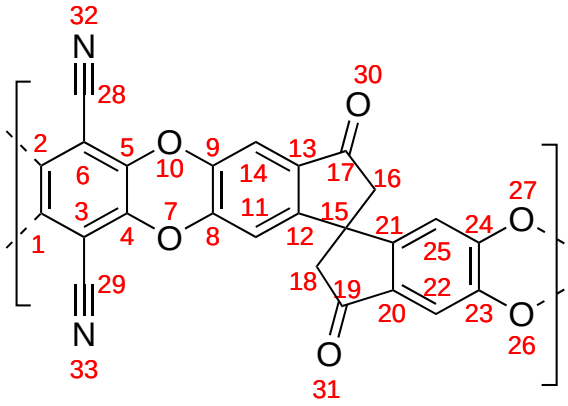

Figure S2: The chemical structure of PIM-1c.

Table S3: Simulation details of PIM-1c.

(a) Porosity properties of the PIM-1c at all swellings

swelling (%)	SA_{geo} (m^2g^{-1})	L (Å)	φ (cm^3g^{-1})	ρ_{bulk} (g cm^{-3})
0	505 ± 85	40.8 ± 0.2	0.426 ± 0.017	1.056 ± 0.019
2	562 ± 87	41.1 ± 0.2	0.445 ± 0.017	1.035 ± 0.019
4	649 ± 88	41.4 ± 0.2	0.464 ± 0.017	1.015 ± 0.018
6	704 ± 76	41.6 ± 0.3	0.484 ± 0.018	0.995 ± 0.018
9	817 ± 83	42.0 ± 0.3	0.513 ± 0.018	0.967 ± 0.017
12	942 ± 75	42.4 ± 0.3	0.544 ± 0.019	0.939 ± 0.017
15	1020 ± 54	42.9 ± 0.3	0.574 ± 0.020	0.912 ± 0.016

(b) Details of each simulation box of PIM-1c

sample	No. of United Atoms	M_w (g/mol)
1	3300	43235
2	3300	26105
3	3300	14120
4	3300	28890
5	3300	35271

Table S4: Force field parameters of PIM-1c. Reprinted (adapted) with permission from Larsen et al.[11] Copyright 2011 American Chemical Society.

		GAFF equivalence		TraPPE-UA equivalence		
Atom No.	Atom type	Atom type	Ref.	Atom type	Ref.	Atomic Charge
1, 2, 4, 5	CS0	ca	2	**C**(aro link)	3	0.319062
3, 6	CA0	ca	2	R–**C**(aro)	3	-0.376824
7, 10, 26, 27	OA0	os	2	C(aro)–**O**(aro)–C(aro)	4	-0.108096
9, 8, 23, 24	CS0	ca	2	**C**(aro link)	3	-0.193873
11, 14, 22, 25	CA1	ca	2	**CH**(aro)	3	0.318224
12, 13, 20, 21	CA0	ca	2	R–**C**(aro)	3	-0.131754
15	CH0	c3	2	**C**	6	0.0
17, 19	CP0	c2	2	**C**(sp^2)	8	0.314104
16, 18	CH2	c3	2	**CH_2**	5	0.192322
28, 29	CL0	c1	2	**C**(*sp*)	7	0.302473
32, 33	NL0	n1	2	**N**(nitrile)	7	-0.368858
30, 31	OK0	oc	2	**O**(ketone)	9	-0.470344

2.3 sPIM-1

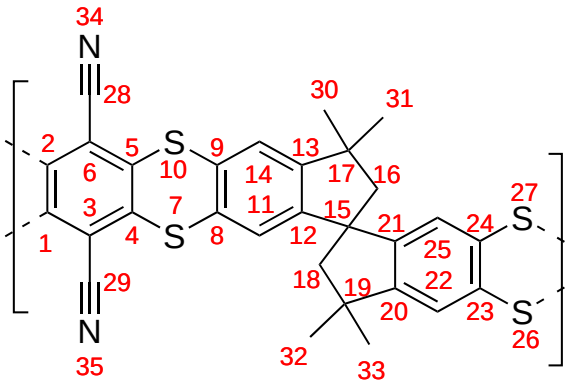

Figure S3: The chemical structure of sPIM-1.

Table S5: Simulation details of sPIM-1.

(a) Porosity properties of the sPIM-1 at all swellings

swelling (%)	SA_{geo} (m^2g^{-1})	L (Å)	φ (cm^3g^{-1})	ρ_{bulk} (g cm^{-3})
0	282 ± 65	51.1 ± 1.4	0.354 ± 0.015	1.055 ± 0.016
2	328 ± 71	51.4 ± 1.4	0.372 ± 0.015	1.034 ± 0.016
4	384 ± 60	51.8 ± 1.4	0.392 ± 0.015	1.014 ± 0.016
6	443 ± 72	52.1 ± 1.5	0.410 ± 0.016	0.995 ± 0.016
9	557 ± 73	52.6 ± 1.5	0.440 ± 0.016	0.966 ± 0.016
12	681 ± 73	53.2 ± 1.5	0.470 ± 0.017	0.938 ± 0.017
15	771 ± 62	53.7 ± 1.5	0.501 ± 0.017	0.912 ± 0.014

(b) Details of each simulation box of sPIM-1

sample	No. of United Atoms	M_w (g/mol)
1	6055	11589
2	5005	20802
3	5355	11932
4	6090	17781
5	5845	16713

Table S6: Force field parameters of sPIM-1. Reprinted (adapted) with permission from Hart et al.[13] Copyright 2013 American Chemical Society.

		GAFF equivalence		TraPPE-UA equivalence		
Atom No.	Atom type	Atom type	Ref.	Atom type	Ref.	Atomic Charge
1, 2, 4, 5	CS0	ca	2	**C**(aro link)	3	-0.1081570
3, 6	CA0	ca	2	R–**C**(aro)	3	0.3077860
7, 10, 26, 27	S20	ss	2	C(aro)–**S**(aro)–C(aro)	4	0.0043710
9, 8, 23, 24	CS0	ca	2	**C**(aro link)	3	-0.1892980
11, 14, 22, 25	CA1	ca	2	**CH**(aro)	3	0.3261810
12, 13, 20, 21	CA0	ca	2	R–**C**(aro)	3	-0.2400730
15	CH0	c3	2	**C**	6	0.1865893
17, 19	CH0	c3	2	**C**	6	0.1865893
16, 18	CH2	c3	2	**CH_2**	5	0.0086540
28, 29	CL0	c1	2	**C**(*sp*)	7	0.2149250
34, 35	NL0	n1	2	**N**(nitrile)	7	-0.3972980
30, 31, 32, 33	CH3	c3	2	**CH_3**	5	0.0

2.4 PIM-SBF

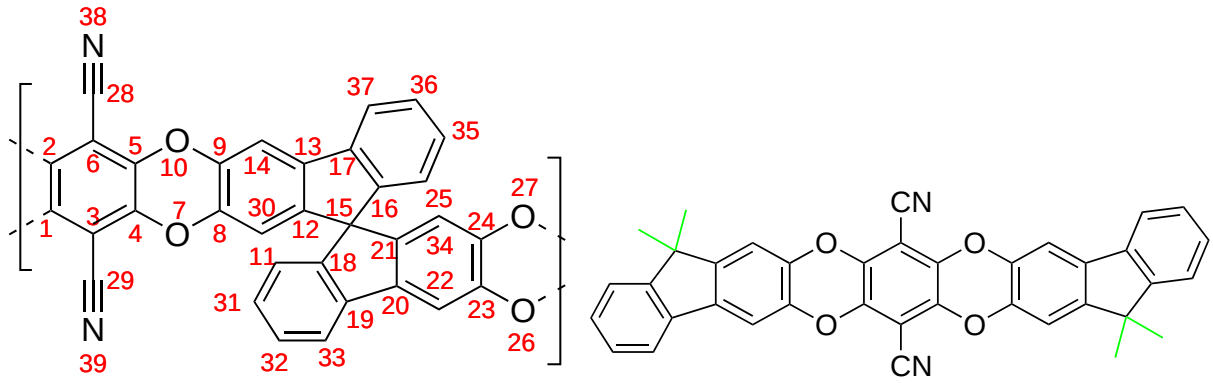

Figure S4: The chemical structure (left) and symmetric repeat unit (right) of PIM-SBF.

Table S7: Simulation details of PIM-SBF.

(a) Porosity properties of the PIM-SBF at all swellings

swelling (%)	SA_{geo} (m^2g^{-1})	L (Å)	φ (cm^3g^{-1})	ρ_{bulk} (g cm^{-3})
0	549 ± 46	43.4 ± 0.1	0.446 ± 0.009	1.019 ± 0.009
2	613 ± 37	43.7 ± 0.1	0.465 ± 0.009	0.999 ± 0.009
4	669 ± 76	43.9 ± 0.1	0.485 ± 0.009	0.979 ± 0.009
6	773 ± 42	44.2 ± 0.1	0.505 ± 0.009	0.960 ± 0.008
9	871 ± 47	44.7 ± 0.1	0.536 ± 0.010	0.932 ± 0.008
12	988 ± 39	45.1 ± 0.1	0.568 ± 0.010	0.906 ± 0.008
15	1089 ± 71	45.5 ± 0.1	0.600 ± 0.010	0.880 ± 0.010

(b) Details of each simulation box of PIM-SBF

sample	No. of United Atoms	M_w (g/mol)
1	3900	9739
2	3900	14183
3	3900	7697
4	3900	12292
5	3900	6957

Table S8: Force field parameters of PIM-SBF from this work.

		GAFF equivalence		TraPPE-UA equivalence		
Atom No.	Atom type	Atom type	Ref.	Atom type	Ref.	Atomic Charge
1, 5	CS0	ca	2	**C**(aro link)	3	0.153146
2, 4	CS0	ca	2	**C**(aro link)	3	0.195742
3, 6	CA0	ca	2	R–**C**(aro)	3	-0.121670
10, 26	OA0	os	2	C(aro)–**O**(aro)–C(aro)	4	-0.234017
7, 27	OA0	os	2	C(aro)–**O**(aro)–C(aro)	4	-0.245171
8, 24	CS0	ca	2	**C**(aro link)	3	0.183783
9, 23	CS0	ca	2	**C**(aro link)	3	0.216742
14, 22	CA1	ca	2	**CH**(aro)	3	-0.304324
30, 34	CA1	ca	2	**CH**(aro)	3	-0.314783
13, 20	CA0	ca	2	R–**C**(aro)	3	-0.0155590
12, 21	CA0	ca	2	R–**C**(aro)	3	0.0559840
15	CH0	c3	2	**C**	6	0.0834720
16, 18	CA0	ca	2	R–**C**(aro)	3	0.117060
17, 19	CA0	ca	2	R–**C**(aro)	3	0.0672310
11, 25	CA1	ca	2	**CH**(aro)	3	-0.0822140
31, 35	CA1	ca	2	**CH**(aro)	3	0.0130180
32, 36	CA1	ca	2	**CH**(aro)	3	-0.0140310
33, 37	CA1	ca	2	**CH**(aro)	3	-0.0336580
28, 29	CL0	c1	2	**C**(*sp*)	7	0.322237
38, 39	NL0	n1	2	**N**(nitrile)	7	-0.411804

2.5 PIM-SBF-Me

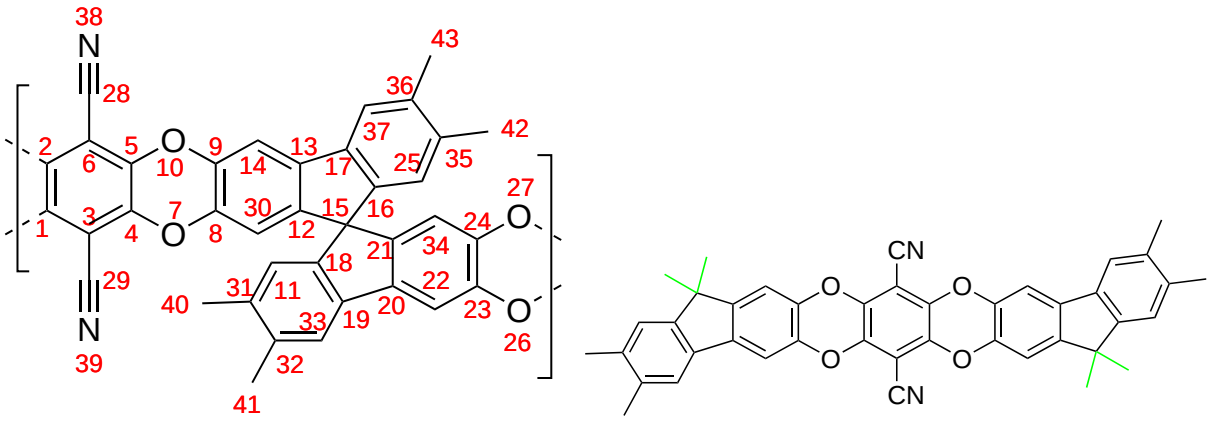

Figure S5: The chemical structure (left) and symmetric repeat unit (right) of PIM-SBF-Me.

Table S9: Simulation details of PIM-SBF-Me.

(a) Porosity properties of the SBF-Me at all swellings

swelling (%)	SA_{geo} (m^2g^{-1})	L (Å)	φ (cm^3g^{-1})	ρ_{bulk} (g cm^{-3})
0	864 ± 155	46.7 ± 0.5	0.550 ± 0.038	0.907 ± 0.031
2	932 ± 139	47.0 ± 0.5	0.571 ± 0.039	0.889 ± 0.031
4	1012 ±148	47.3 ± 0.5	0.594 ± 0.040	0.872 ± 0.030
6	1098 ±149	47.7 ± 0.5	0.617 ± 0.040	0.855 ± 0.029
9	1226 ±128	48.1 ± 0.6	0.652 ± 0.042	0.830 ± 0.028
12	1337 ±130	48.6 ± 0.6	0.687 ± 0.043	0.806 ± 0.028
15	1451 ±109	49.1 ± 0.6	0.723 ± 0.044	0.783 ± 0.027

(b) Details of each simulation box of SBF-Me

sample	No. of United Atoms	M_w (g/mol)
1	4300	16230
2	4300	9907
3	4300	10497
4	4300	22742
5	4300	9740

Table S10: Force field parameters of PIM-SBF-Me from this work.

		GAFF equivalence		TraPPE-UA equivalence		
Atom No.	Atom type	Atom type	Ref.	Atom type	Ref.	Atomic Charge
1, 5	CS0	ca	2	**C**(aro link)	3	0.166935
2, 4	CS0	ca	2	**C**(aro link)	3	0.174542
3, 6	CA0	ca	2	R–**C**(aro)	3	-0.118530
10, 26	OA0	os	2	C(aro)–**O**(aro)–C(aro)	4	-0.217261
7, 27	OA0	os	2	C(aro)–**O**(aro)–C(aro)	4	-0.244781
8, 24	CS0	ca	2	**C**(aro link)	3	0.234535
9, 23	CS0	ca	2	**C**(aro link)	3	0.165025
14, 22	CA1	ca	2	**CH**(aro)	3	-0.112199
30, 34	CA1	ca	2	**CH**(aro)	3	-0.157085
13, 20	CA0	ca	2	R–**C**(aro)	3	0.0554840
12, 21	CA0	ca	2	R–**C**(aro)	3	0.0593660
15	CH0	c3	2	**C**	6	0.0971560
16, 18	CA0	ca	2	R–**C**(aro)	3	0.0221620
17, 19	CA0	ca	2	R–**C**(aro)	3	0.0425210
11, 25	CA1	ca	2	**CH**(aro)	3	-0.151034
31, 35	CA0	ca	2	R–**C**(aro)	3	0.111115
32, 36	CA0	ca	2	R–**C**(aro)	3	0.0829760
33, 37	CA1	ca	2	**CH**(aro)	3	-0.120762
28, 29	CL0	c1	2	**C**(*sp*)	7	0.315785
38, 39	NL0	n1	2	**N**(nitrile)	7	-0.410415
41	CH3	c3	2	**CH**$_3$	5	0.00167400
42	CH3	c3	2	**CH**$_3$	5	0.00360200
43	CH3	c3	2	**CH**$_3$	5	0.000908000
40	CH3	c3	2	**CH**$_3$	5	0.00275000

3 Effective Swelling

```
# Dilation step.
change_box all x scale 1.05 y scale 1.05 z scale 1.05 remap units box

# Equilibration part 1; NVT at 600 K
fix               1 all nvt temp 600 600 100.0
velocity          all create 600 58447419
run               100000
unfix             1

# Equilibration part 2; NVT at 300 K
fix               2 all nvt temp 300 300 100.0
velocity          all create 300 58447419
run               50000
unfix             2
```

The above script can be amended to any LAMMPS input script (e.g., the 21-step compression scheme found in Abbott et al.[10]) to employ the effective swelling procedure used in this work. The above example is using a dilation factor (f) of 1.05, which corresponds to $\sim$ 15 % swelling. To use this script for another swelling percent, the dilation factor should be changed accordingly.

4 Characterization

Show below are the characterization of all PIMs for: spirocenter-spirocenter radial distribution functions, structure factors, pore size distributions, nitrogen adsorption isotherms at 77 K.

4.1 Radial distribution functions

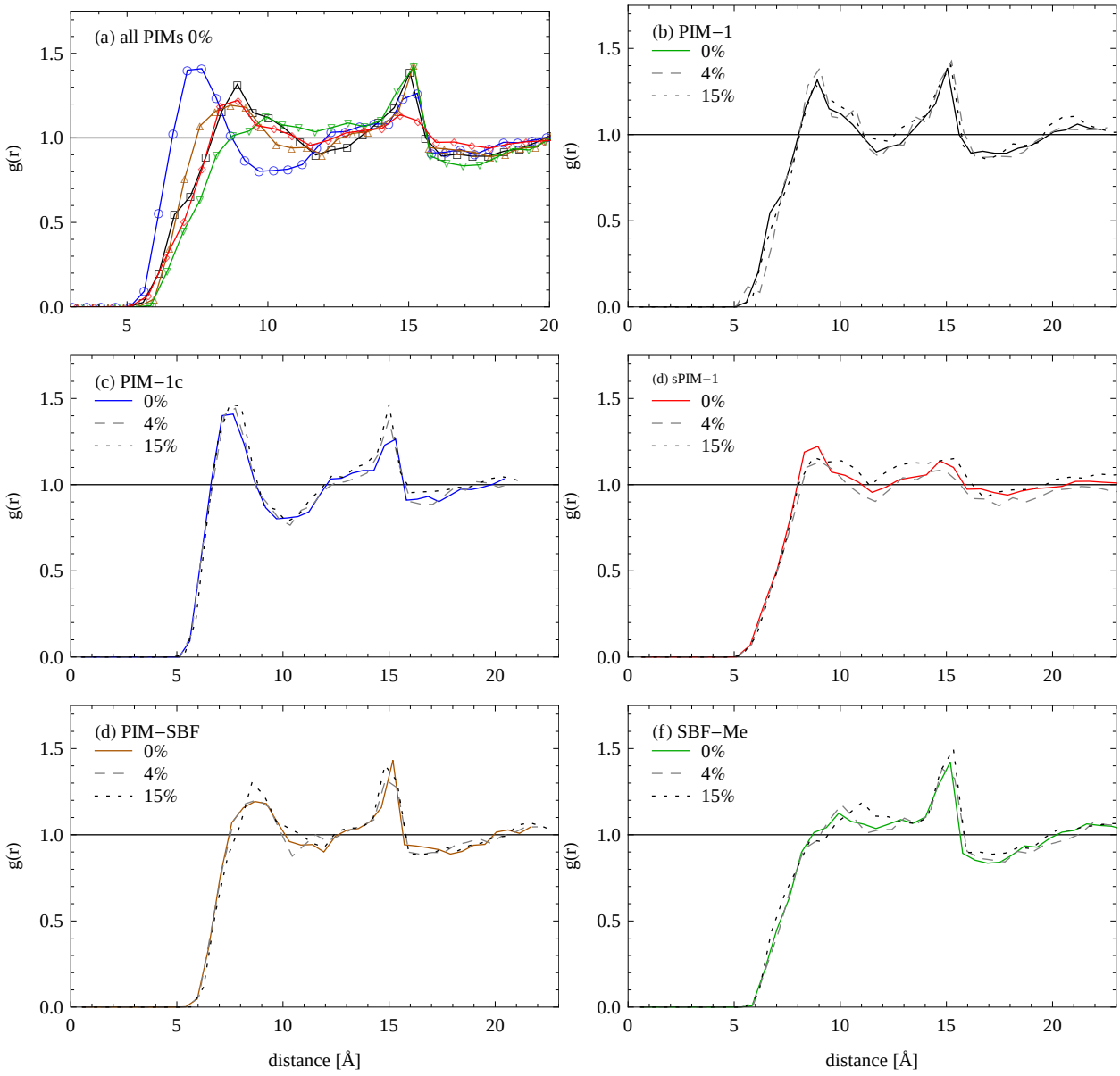

Figure S6: The spirocenter–spirocenter radial distribution function of (a) all PIMs at 0%, and 0%, 4%, and 15% of (b) PIM-1, (c) PIM-1c, (d) sPIM-1, (e) PIM-SBF, and (f) PIM-SBF-Me. Each curve is the average of the simulated sample set.

4.2 Structure factors

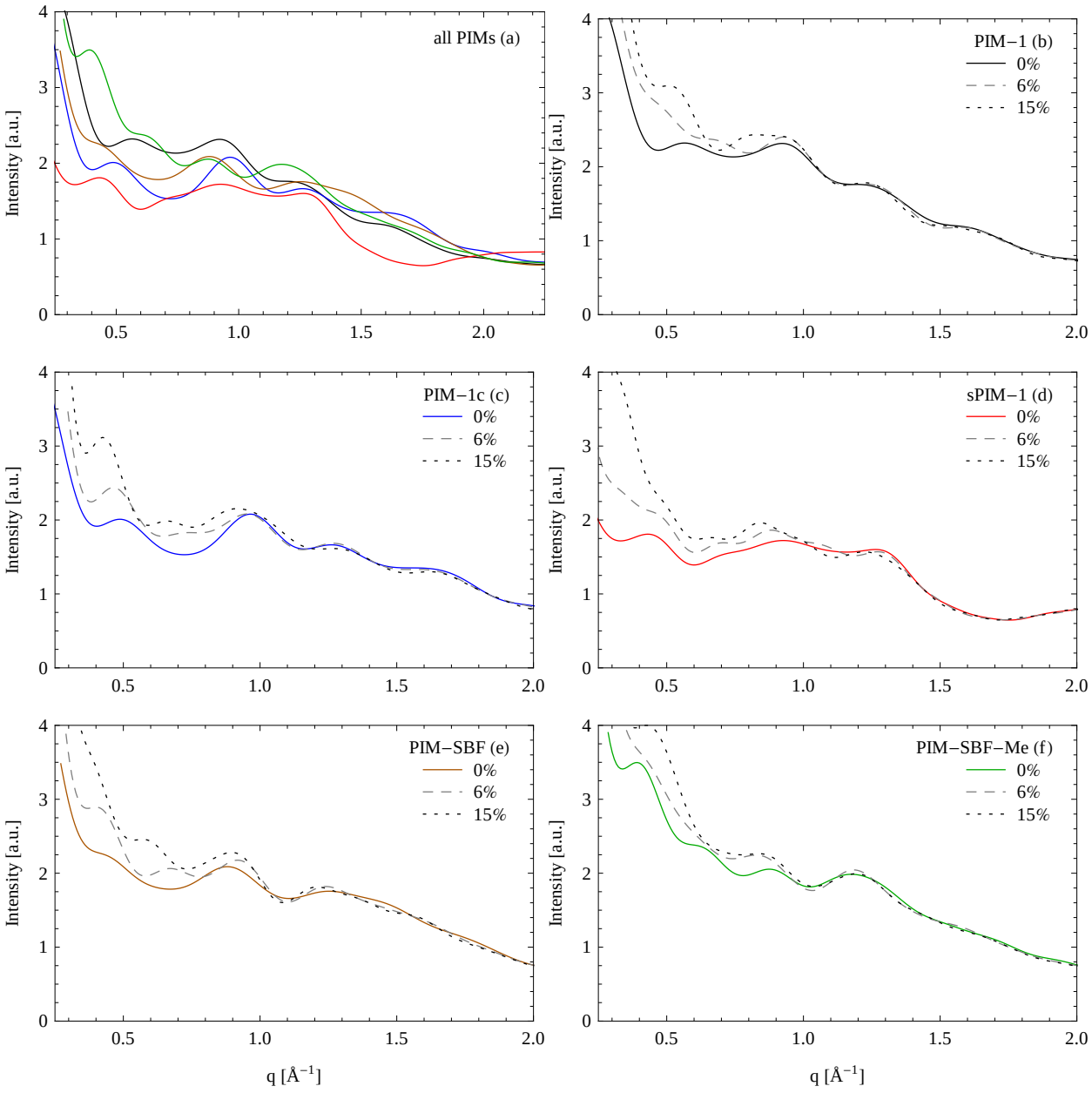

Figure S7: The structure factors of (a) all PIMs at 0%, and 0%, 6%, and 15% of (b) PIM-1, (c) PIM-1c, (d) sPIM-1, (e) PIM-SBF, and (f) PIM-SBF-Me. Each curve is the average of the simulated sample set.

4.3 Pore Size Distributions

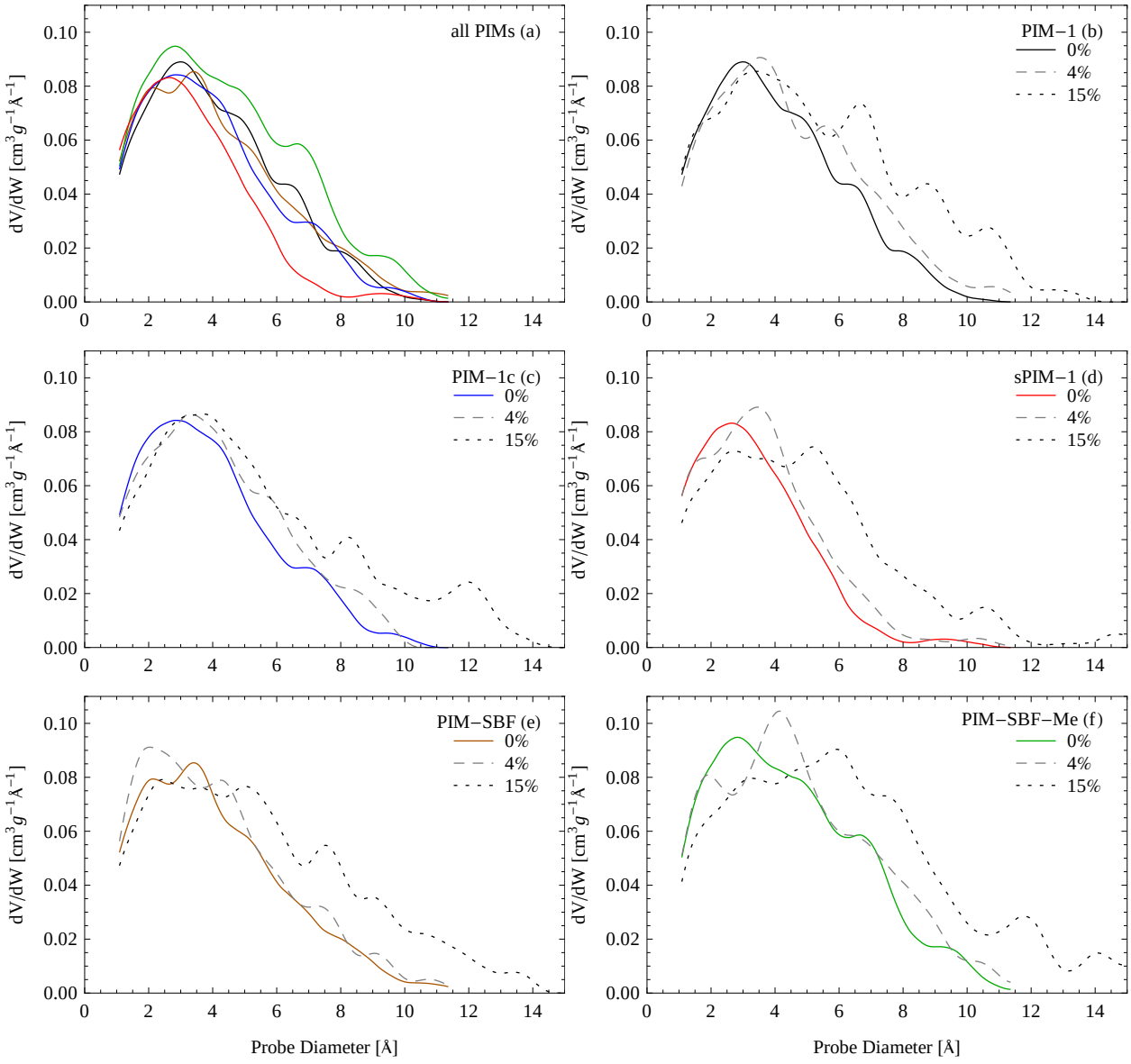

Figure S8: The pore size distribution curves of (a) all PIMs at 0%, and 0%, 4%, and 15% of (b) PIM-1, (c) PIM-1c, (d) sPIM-1, (e) PIM-SBF, and (f) PIM-SBF-Me. Each curve is the average of the simulated sample set.

4.4 Curling Angle Distributions

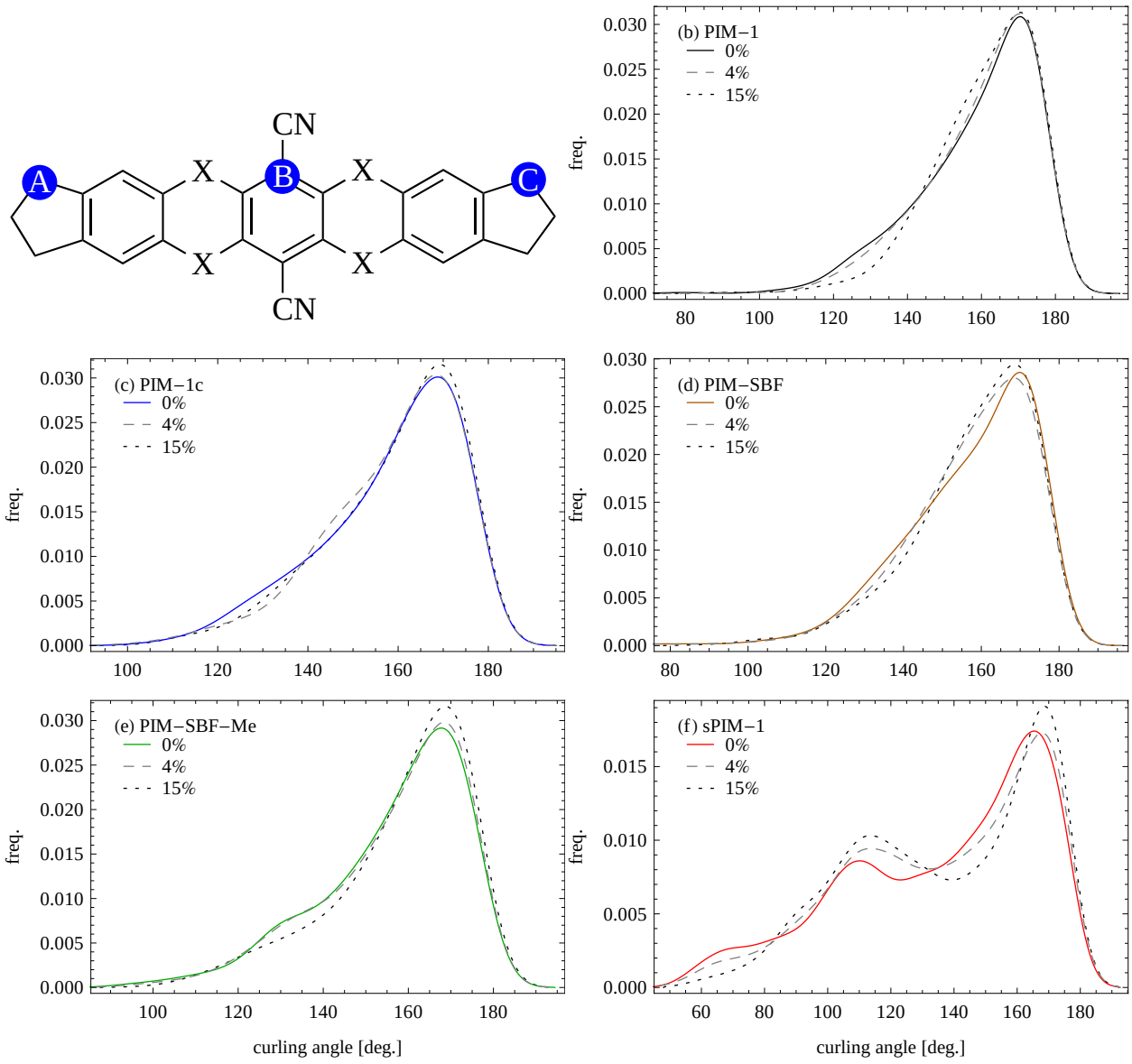

Figure S9: The backbone 'curling' angle distributions, as define in (a) by the $\angle ABC$, for 0%, 4%, and 15% of (b) PIM-1, (c) PIM-1c, (d) sPIM-1, (e) PIM-SBF, and (f) PIM-SBF-Me. Averaged over 10 snapshots of a 500 ps NVT MD simulation.

4.5 Spiro-Angle Distributions

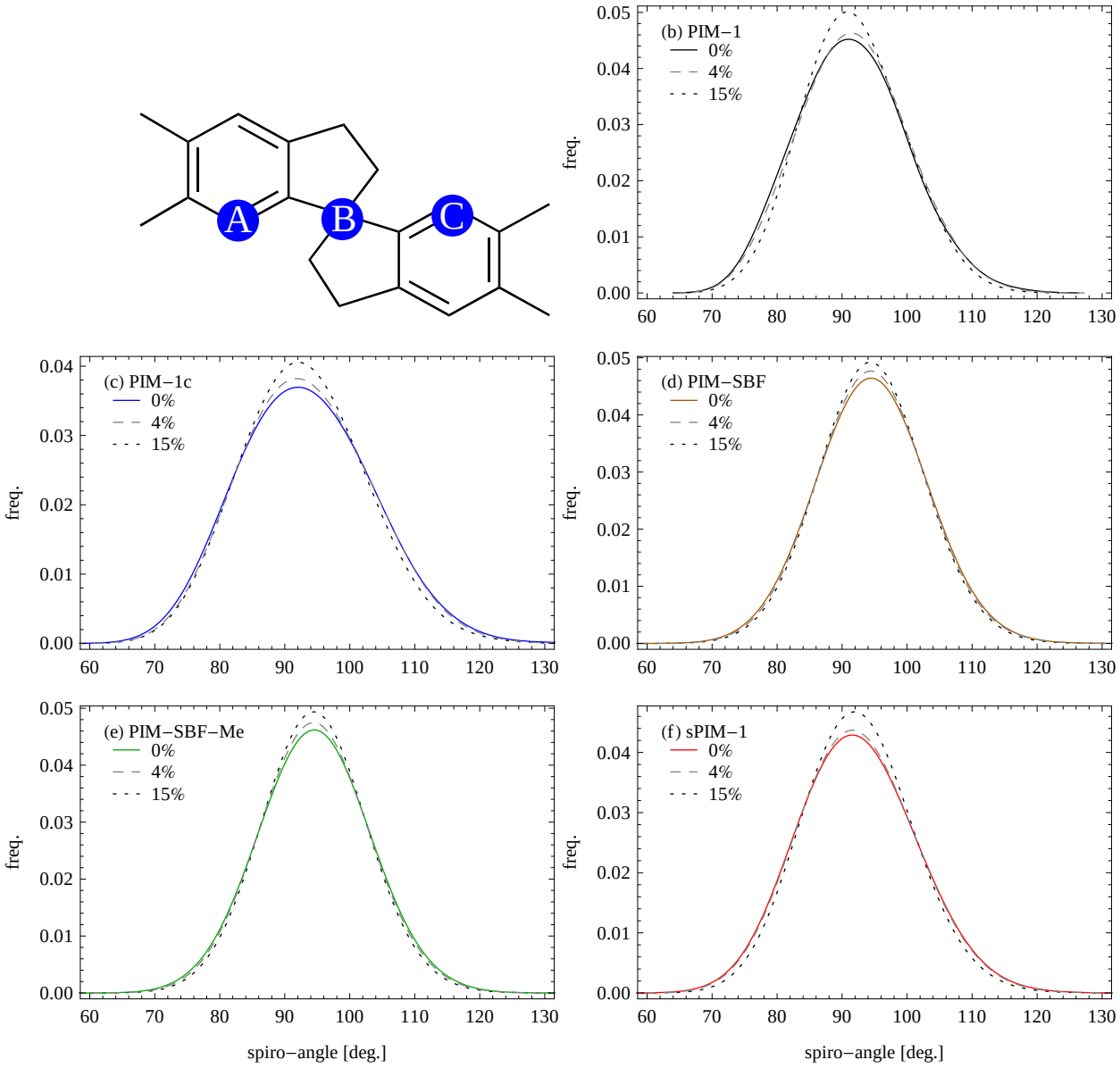

Figure S10: The spirocenter 'spiro-angle' distributions, as define in (a) by the $\angle ABC$, for 0%, 4%, and 15% of (b) PIM-1, (c) PIM-1c, (d) sPIM-1, (e) PIM-SBF, and (f) PIM-SBF-Me. Averaged over 10 snapshots of a 500 ps NVT MD simulation.

4.6 N_2 adsorption

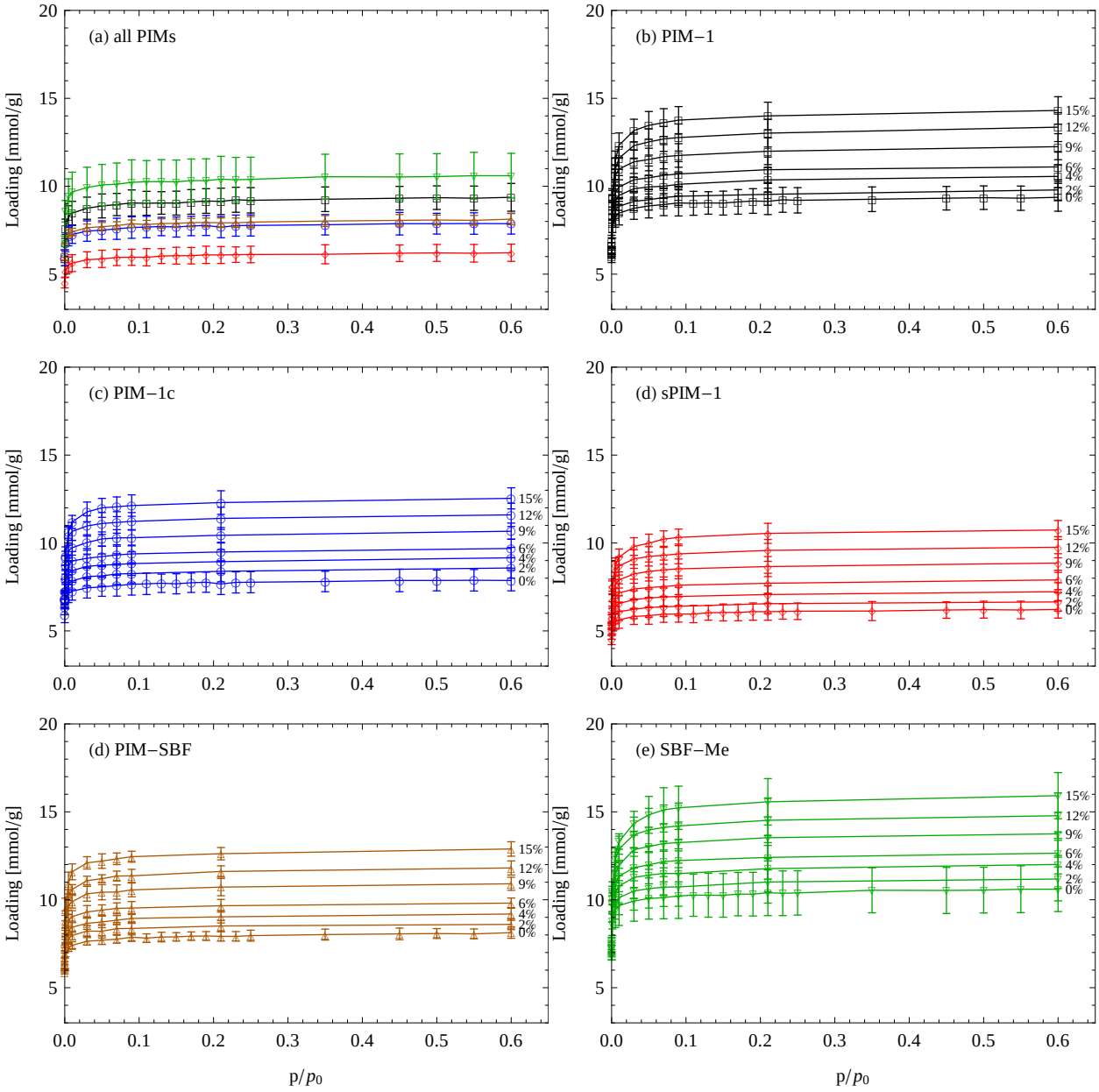

Figure S11: The N_2 adsorption isotherm of the simulated samples of (a) all PIMs at 0%, (b) PIM-1, (c) PIM-1c, (d) sPIM-1, (e) PIM-SBF, and (f) PIM-SBF-Me. All isotherms are represented as the average and standard deviation of the five simulation samples in each sample set.

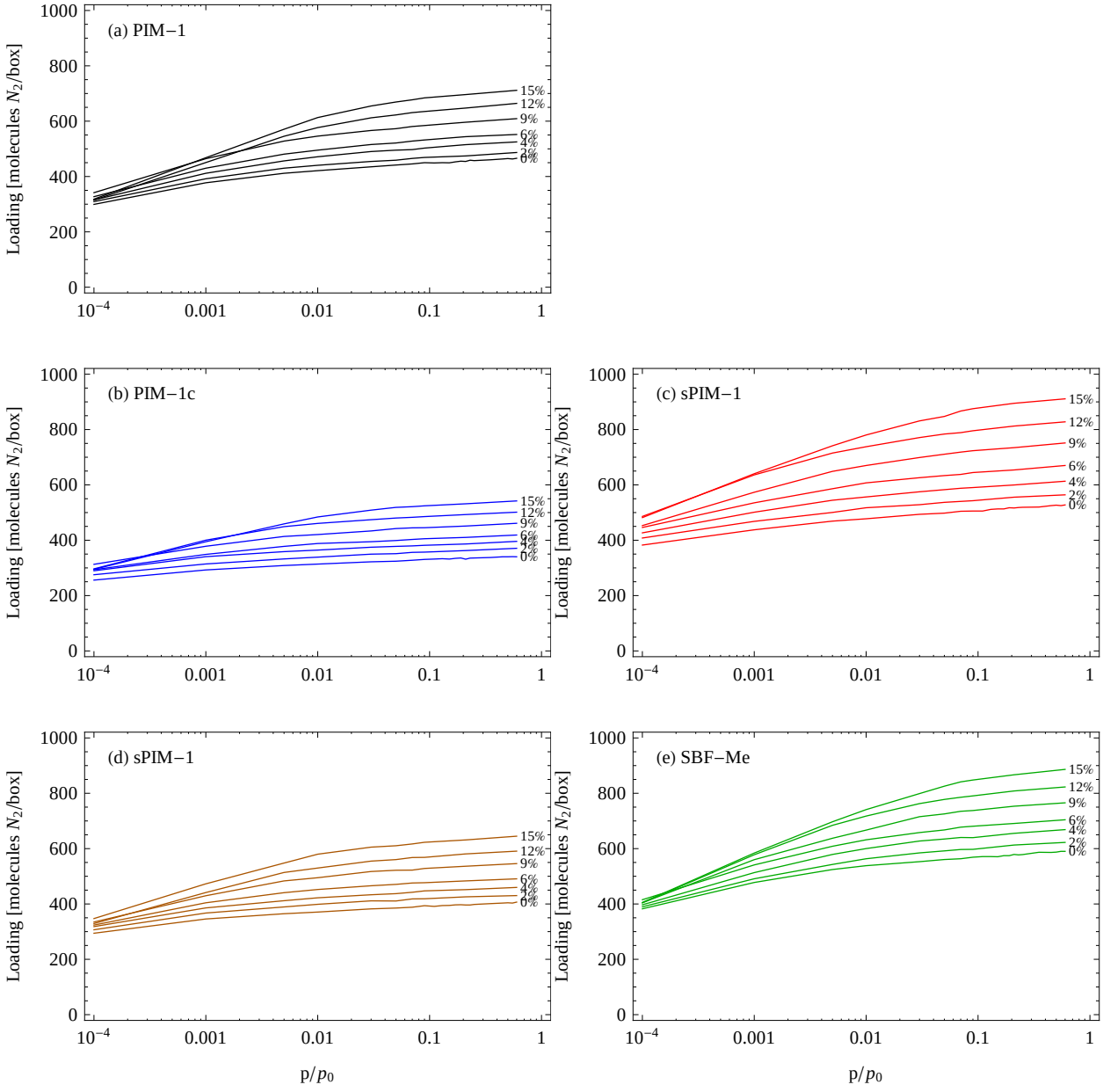

Figure S12: The number of molecules of N_2 adsorbed per simulation box of the simulated samples of (a) PIM-1, (b) PIM-1c, (c) sPIM-1, (d) PIM-SBF, and (e) PIM-SBF-Me. All isotherms are represented as the average of the five simulation samples in each sample set.

4.7 N_2 adsorption enthalpy

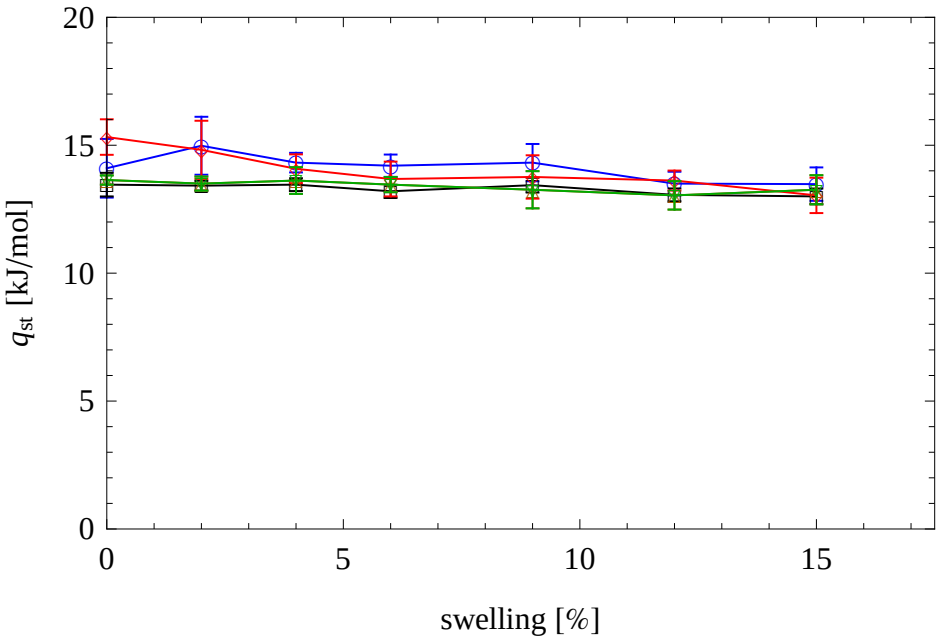

Figure S13: The N_2 enthalpy of adsorption of the simulated samples calculated at the lowest pressure (0.0001 bar) as a function of swelling percent for: PIM-1 (□), PIM-1c (○), PIM-SBF (△), PIM-SBF-Me (▽), sPIM-1 (◇). All values are represented as the average and standard deviation of the five simulation samples in each sample set.

References

(1) Bayly, C. I.; Cieplak, P.; Cornell, W. D.; Kollman, P. A. *J. Phys. Chem.* **1993**, *97*, 10269–10280.

(2) Wang, J.; Wolf, R. M.; Caldwell, J. W.; Kollman, P. A.; Case, D. A. *J. Comput. Chem.* **2004**, *25*, 1157–74.

(3) Wick, C. D.; Martin, M. G.; Siepmann, J. I. *J. Phys. Chem. B* **2000**, *104*, 8008–8016.

(4) Rai, N.; Siepmann, J. I. *J. Phys. Chem. B* **2007**, *111*, 10790–10799.

(5) Martin, M. G.; Siepmann, J. I. *J. Phys. Chem. B* **1998**, *102*, 2569–2577.

(6) Martin, M. G.; Siepmann, J. I. *J. Phys. Chem. B* **1999**, *103*, 4508–4517.

(7) Wick, C. D.; Stubbs, J. M.; Rai, N.; Siepmann, J. I. *J. Phys. Chem. B* **2005**, *109*, 18974–18982.

(8) Stubbs, J. M.; Potoff, J. J.; Siepmann, J. I. *J. Phys. Chem. B* **2004**, *108*, 17596–17605.

(9) Lee, J.-S.; Wick, C. D.; Stubbs, J. M.; Siepmann, J. I. *Mol. Phys.* **2005**, *103*, 99–104.

(10) Abbott, L. J.; Hart, K. E.; Colina, C. M. *Theor. Chem. Acc.* **2013**, *132*, 1334.

(11) Larsen, G. S.; Lin, P.; Hart, K. E.; Colina, C. M. *Macromolecules* **2011**, *44*, 6944–6951.

(12) Hart, K. E.; Abbott, L. J.; Colina, C. M. *Mol. Simul.* **2013**, *39*, 397–404.

(13) Hart, K. E.; Abbott, L. J.; McKeown, N. B.; Colina, C. M. *Macromolecules 46*, 5371–5380.

(14) Abbott, L. J.; McDermott, A. G.; Del Regno, A.; Taylor, R. G. D.; Bezzu, C. G.; Msayib, K. J.; McKeown, N. B.; Siperstein, F. R.; Runt, J.; Colina, C. M. *J. Phys. Chem. B* **2013**, *117*, 355–364.

(15) Del Regno, A.; Siperstein, F. R.; Taylor, R. G. D.; McKeown, N. B. *Microporous Mesoporous Mater.* **2013**, *176*, 55–63.

(16) Plimpton, S. *J. Comput. Phys.* **1995**, *117*, 1–19.